







Research Article

Optimum Green Synthesis of Silver Nanoparticles with the Highest Antibacterial Activity against *Streptococcus mutans* Biofilm

Azam Chahardoli ¹, Mohsen Safaei ^{2,3}, Mohammad Salmani Mobarakeh ²,
Nima Fallahnia ⁴, Behnam Fatehi ⁴, Mohammad Moslem Imani ⁵,
and Amin Golshah ⁵

¹Department of Biology, Faculty of Science, Razi University, Kermanshah, Iran

²Advanced Dental Sciences Research Center, School of Dentistry, Kermanshah University of Medical Sciences, Kermanshah, Iran

³Division of Dental Biomaterials, School of Dentistry, Kermanshah University of Medical Sciences, Kermanshah, Iran

⁴Students Research Committee, Kermanshah University of Medical Sciences, Kermanshah, Iran

⁵Department of Orthodontics, School of Dentistry, Kermanshah University of Medical Sciences, Kermanshah, Iran

Correspondence should be addressed to Mohsen Safaei; mohsen_safaei@yahoo.com

Received 14 April 2022; Accepted 29 August 2022; Published 19 September 2022

Academic Editor: H C Ananda Murthy

Copyright © 2022 Azam Chahardoli et al. This is an open access article distributed under the Creative Commons Attribution License, which permits unrestricted use, distribution, and reproduction in any medium, provided the original work is properly cited.

Nowadays, resistance to antibiotics has developed in bacterial microorganisms related to dental and oral infections, leading to major problems in public health. Using nanoparticles, particularly silver nanoparticles (AgNPs) may offer a new strategy for the prevention and treatment of dental infections. In the current study, AgNPs were synthesized using *Halomonas elongata* at different conditions according to nine experiments designed by the Taguchi method, and their antibacterial effects were investigated on a *Streptococcus mutans* biofilm. The effects of three factors, including silver nitrate (AgNO₃) concentration, incubation time, and temperature at three different levels, were studied to optimize the synthesis of AgNPs under the designed experiments. Then, the antibacterial effects of these NPs on the *S. mutans* biofilm were examined by the colony-forming unit (CFU) method. According to the results, green-synthesized AgNPs under optimal conditions properly inhibit the formation and growth of the *S. mutans* biofilm. Furthermore, different analyses were applied to investigate the formation, structural, and morphological properties of the green-synthesized AgNPs under optimum conditions. The obtained results of this study indicated that the green-synthesized AgNPs could be a promising antimicrobial agent in the dental and medicinal industry.

1. Introduction

Despite significant therapeutic advances in recent decades, no effective treatment has been found for autoimmune diseases, cancer, and microbial infections [1–3]. The emergence of drug-resistant bacteria has become a main global health concern because it is hard to control these pathogenic strains using commonly available antibiotics [4, 5]. According to a report from the World Health Organization (WHO), resistance to antibiotics has also developed in bacterial microorganisms

related to dental and oral infections [6]. For example, in a study on antibiotic-resistant bacteria, such as oral *Streptococci* from active dental infections, it was shown that 45.9% of *S. mutans* were resistant to clindamycin and moxifloxacin [7]. There are several microorganisms in the oral cavity that may cause oral diseases including caries, periodontitis, and other dental disorders [8]. The majority of dental diseases are caused by the formation of plaque biofilms by a community of bacteria or fungi that protects pathogenic microorganisms from foreign drugs and allows them to escape the host's defenses [9].

Therefore, there is an urgent need to develop and produce new antibacterial agents to control bacterial infections [10]. Due to their large surface area and high charge density, nanoparticles (NPs) may offer a new strategy for the prevention and treatment of dental infections. This is because they interact more with the negatively charged surface of bacterial cells, thereby increasing their antimicrobial activity [8–11].

Among NPs, silver nanoparticles (AgNPs) were introduced as a strong antimicrobial and antibiofilm agent against pathogenic microorganisms, including viruses, bacteria, and eukaryotic microorganisms [4]. Various expensive and environmentally hazardous physical and chemical methods can be used to synthesize AgNPs [12]. Recently, the biological synthesis of NPs using renewable materials (microorganisms and plants), as a safe alternative method, has received huge attention [13]. Green-synthesized NPs have received more attention due to reducing the usage of chemicals, the advantage of ecological friendliness, easy and cost-effective synthesis, energy-efficient approach, etc. [14, 15]. Microorganisms possess the capability to synthesize NPs [16]. Bacteria (the most commonly used microorganisms) have an extraordinary ability to reduce heavy metal ions and are hence considered one of the best candidates for the synthesis of NPs [17]. In recent research, different bacteria such as *Escherichia coli*, *Bacillus subtilis*, *Lactobacillus rhamnosus*, and *Leucas aspera* have been applied to the synthesis of AgNPs [18–21]. Therefore, the present study is aimed at the green synthesis of AgNPs using *Halomonas elongata* as a nonpathogenic Gram-negative proteobacterium at optimum conditions. In addition to the synthesis and characterization of NPs, their highest antibacterial activity against the *S. mutans* biofilm as the main cause of dental caries was investigated in this study.

2. Materials and Methods

2.1. Synthesis of AgNPs using *H. elongata*. Prior to the synthesis of NPs, the bacterial source of *H. elongata* (IBRC-M 10433; Iranian biological resource center) was obtained from the bacterial archive. The obtained strain was cultured in an appropriate sterilized medium, containing glucose (0.2 g), NaCl (3 g), K_2HPO_4 (0.028 g), and $FeSO_4$ (0.0001 g) in an Erlenmeyer flask, and then was incubated at 37°C for 48 h. After the incubation time, the bacteria solution was isolated from the culture medium by centrifugation at 5000 rpm for 10 min. The supernatant was stored for the synthesis of AgNPs, which was optimized using the Taguchi method. According to this method, nine experiments were designed based on different factors, including silver nitrate ($AgNO_3$) concentrations (0.3, 0.6, and 0.9 mg/mL), incubation times (48, 72, and 96 h), and incubation temperatures (27, 32, and 37°C). The synthesis process was started by adding 0.5 mL of the bacterial supernatant to the $AgNO_3$ solution at different concentrations. Then, the reaction solutions were shaken (120 rpm) in an incubator shaker under different temperatures and incubation times. A control sample without bacteria was placed under the same conditions. After the reaction was completed, the formed AgNPs were separated by centrifugation for 15 min at 5000 rpm.

2.2. Antibacterial Effects. The antimicrobial effects of the green-synthesized AgNPs against *S. mutans* were evaluated using colony-forming unit (CFU) methods. From the bacterial archive of the Iranian biological resource center, a strain of *S. mutans* (ATCC 35668) was obtained. *S. mutans* was cultured on brain heart infusion agar (BHIA) medium for 24 h to prepare a new colony. After that, a bacterial suspension (0.5 McFarland) was prepared from the produced colony.

S. mutans was cultured overnight in a BHI broth medium at 37°C to form a bacterial biofilm. Then, the bacterial suspension was inoculated to a 96-well plate and incubated at 37°C for 72 h. Daily, the culture medium was replaced with a fresh BHI broth containing 2% sucrose and 1% mannose. After biofilm formation, it was washed three times with PBS to remove planktonic *S. mutans*. The synthesized AgNPs were then added to each well according to nine experiments designed by the Taguchi method, and the prepared plates were incubated for 24 h. To measure the viable cells in the biofilms, the unattached cells were removed from the wells after incubation at 37°C for 24 h. The adhering cells on the wells were washed (three times), and the resulting suspension was then homogenized using vortex in PBS buffer for 2 min. To test the CFU, the bacterial suspensions were diluted 10 times with BHI broth as a serial dilution. Then, each dilution was cultured on BHIA plates and incubated at 37°C for 24 h. After the incubation time, the number of colonies was counted for nine experiments. All tests were repeated three times.

2.3. Characterization. The characterization of green-synthesized AgNPs was performed using different analysis techniques, including UV-vis (ultraviolet-visible spectrophotometry), FTIR (Fourier transform infrared spectroscopy), XRD (X-ray powder diffraction), FE-SEM (field emission scanning electron microscopy), EDX (energy dispersive X-ray spectroscopy), and TEM (transmission electron microscopy). UV-vis analysis was used to track the bioreduction of silver ions to AgNPs in the wavelength range of 200–800 nm (Thermo Fisher Scientific Company, Wilmington, USA). FTIR spectroscopy between 400 and 4000 cm^{-1} was used to determine the role of functional groups in the synthesis of AgNPs (Thermo Fisher Scientific Company, Wilmington, USA). To determine the crystalline structure of the green-synthesized NPs, an XRD analysis (PHILIPS's PW1730) was performed in the range of 20–80°. The morphology and size of the formed NPs were determined by a field emission scanning electron microscope (FESEM) (TESCAN Company, MIRA III model, Brno, Czech Republic) and TEM (CM120, Philips Company, Eindhoven, Netherlands) analyses. The elemental composition of the synthesized NPs was determined using the EDX analysis.

3. Results and Discussion

3.1. Antibacterial Analysis. To optimize the synthesis of AgNPs with the most potent antibacterial properties, nine Taguchi experiments were designed. Table 1 summarizes the effects of green-synthesized AgNPs under various conditions on the growth inhibition of *S. mutans* biofilms. According to

TABLE 1: Taguchi design of experiments and bacterial growth inhibition rate of green-synthesized AgNPs.

Experiment	AgNO ₃ concentration (mg/mL)			Incubation temperature (°C)			Incubation time (h)			Bacterial viability rate (Log10 CFU/mL)
	0.3	0.6	0.9	27	32	37	48	72	96	
1		0.3			27			48		2.91
2		0.3			32			72		0.94
3		0.3			37			96		1.31
4		0.6			27			72		2.17
5		0.6			32			96		0.61
6		0.6			37			48		2.34
7		0.9			27			96		1.44
8		0.9			32			48		1.12
9		0.9			37			72		1.26

TABLE 2: The main effects of different levels of AgNO₃ concentration, incubation temperature, and incubation time on growth inhibition of *S. mutans* biofilm.

Factors	Level 1	Level 2	Level 3
AgNO ₃ concentration (mg/mL)	1.72	1.71	1.27
Incubation temperature (°C)	2.17	0.89	1.64
Incubation time (h)	2.12	1.46	1.12

TABLE 3: The interaction effects of studied factors on growth inhibiting of *S. mutans* biofilm.

Interacting factor pairs	Column	Severity index (%)	Optimum conditions
AgNO ₃ concentration × incubation time	3 × 1	39.13	[3, 2]
Incubation time × incubation temperature	3 × 2	12.17	[3, 2]
Incubation temperature × AgNO ₃ concentration	2 × 1	8.91	[2, 2]

TABLE 4: The analysis of variance of factors affecting the growth inhibition of *S. mutans* biofilm.

Factors	DOF	Sum of squares	Variance	F ratio (F)	Pure sum	Percent (%)
AgNO ₃ concentration	2	0.39	0.19	69.14	0.38	8.58
Incubation temperature	2	2.49	1.25	444.77	2.49	55.88
Incubation time	2	1.56	0.78	279.17	1.56	35.03

DOF: degree of freedom.

the results, green-synthesized AgNPs in experiment 5 (0.6 mg/mL of AgNO₃, incubation temperature 32°C, and incubation time 96 h) showed the highest antibacterial effects against *S. mutans*. Log CFUs of AgNPs in experiment 5 were the lowest values among the other groups.

Table 2 presents the effect of AgNO₃ concentrations, incubation temperatures, and incubation times on the growth inhibition of the *S. mutans* biofilm. The outcomes showed that the factors of the AgNO₃ concentration and incubation time at level 3 and incubation temperature at level 2 had the greatest impact on the growth inhibition of the *S. mutans* biofilm.

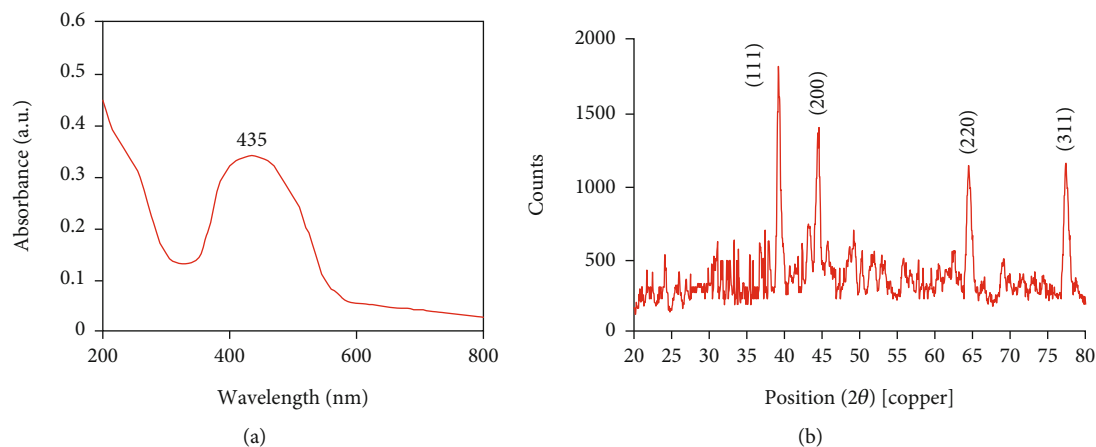
Table 3 presents the interaction between various factors and the inhibition of *S. mutans* biofilm growth. The interac-

tion between AgNO₃ concentration at level 2 and incubation time at level 3 had the greatest effect on the growth inhibition of *S. mutans* biofilm (39.13%). With an intensity index of 12.17%, the interaction between incubation temperature at level 2 and incubation time at level 3 significantly inhibited the growth of *S. mutans* biofilm. The lowest interaction intensity index (8.91%) belonged to the AgNO₃ concentration and incubation temperature at level 2.

Table 4 reveals the analysis of variance for various factors influencing the growth inhibition of *S. mutans* biofilm. The incubation temperature, incubation time, and AgNO₃ concentration with 55.88%, 35.03%, and 8.58% inhibition rates, respectively, showed the greatest effect on the growth inhibition of the *S. mutans* biofilm.

TABLE 5: The optimum conditions for the synthesis of AgNPs with the highest antibiofilm activity.

Factors	Level	Contribution
AgNO ₃ concentration	3	0.29
Incubation temperature	2	0.68
Incubation time	3	0.45
Total contribution from all factors		1.42
Current grand average of performance		1.57
Bacterial growth inhibition at optimum condition		0.15

FIGURE 1: (a) UV-vis spectra and (b) XRD pattern of green-synthesized AgNPs by *H. elongate*.

The optimum conditions for the green synthesis of AgNPs with the maximum antibacterial effects were estimated by analyzing the obtained data from all experiments and investigating the effect of each factor and their interaction (Table 5). Accordingly, the incubation temperature and AgNO₃ concentration showed the highest and the lowest contributions, respectively, to the growth inhibition of the *S. mutans* biofilm. As shown in Table 5, the effect of incubation time on the growth inhibition of the *S. mutans* biofilm is in the middle of the two mentioned factors and is closer to the incubation temperature. It was determined that the third level was ideal for AgNO₃ concentration and incubation time, while the second level was best for incubation temperature. According to the results, it was assessed that the green synthesis of AgNPs under optimal conditions well prevented bacterial activity, which is the closest value to the results of experiment 5 with the lowest Log₁₀ CFU/mL.

The findings of our research are in line with those of Yin et al., who indicated a good antimicrobial effect of green-synthesized spherical AgNPs using epigallocatechin gallate with a diameter of 17 ± 7 nm against the *S. mutans* biofilm [22]. Tavaf et al. showed the antibiofilm activity of green-synthesized AgNPs using *E. coli* (with an average size of 56.1 nm) against *S. mutans* [23].

As reported previously, *S. mutans* is the main oral pathogen causing dental caries and is connected with other systemic diseases, including bacteremia and infective endocarditis. The adhesion of this stain on tooth surfaces

is the main reason for their high cariogenicity [24]. Therefore, green-synthesized AgNPs in the present study with good antibiofilm activity can be an effective agent in the treatment of oral infections or dental caries as well as an alternative way to overcome multi-drug-resistant bacterial infections. The size, ion release capacity, the presence of capping agents, and other physicochemical properties can play a vital role in the antimicrobial activity of AgNPs against various microorganisms such as *S. mutans* [19, 20].

3.2. Physicochemical Characterization of Green-Synthesized AgNPs. In the current study, the bioreduction of Ag⁺ ions to AgNPs using *H. elongata* occurred by changing the color of reaction solutions to brown. The physicochemical properties of green-synthesized AgNPs were analyzed by different techniques such as UV-vis, FTIR, XRD, EDX, FE-SEM, and TEM. Figure 1(a) shows the UV-vis spectrum of AgNPs. The characteristic surface plasmon resonance (SPR) peak for the green-synthesized AgNPs was examined by observing the color change and then by analyzing the maximum absorbance in the range of 400–450 nm, which is evidence of the presence of AgNPs SPR [13]. The maximum absorbance peak of the green-synthesized AgNPs was recorded at 435 nm, which confirmed the production of AgNPs using *H. elongata* strain. The XRD pattern of green-synthesized AgNPs is shown in Figure 1(b). The diffraction peaks at 2θ values of 39.12°, 44.46°, 64.51°, and 77.41° corresponding to reflection peaks of (111), (200), (220), and (311) planes, respectively, revealed

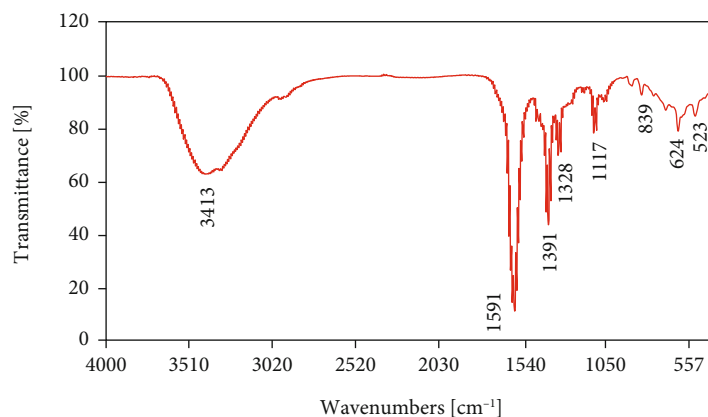


FIGURE 2: FTIR spectrum of green-synthesized AgNPs by *H. elongate*.

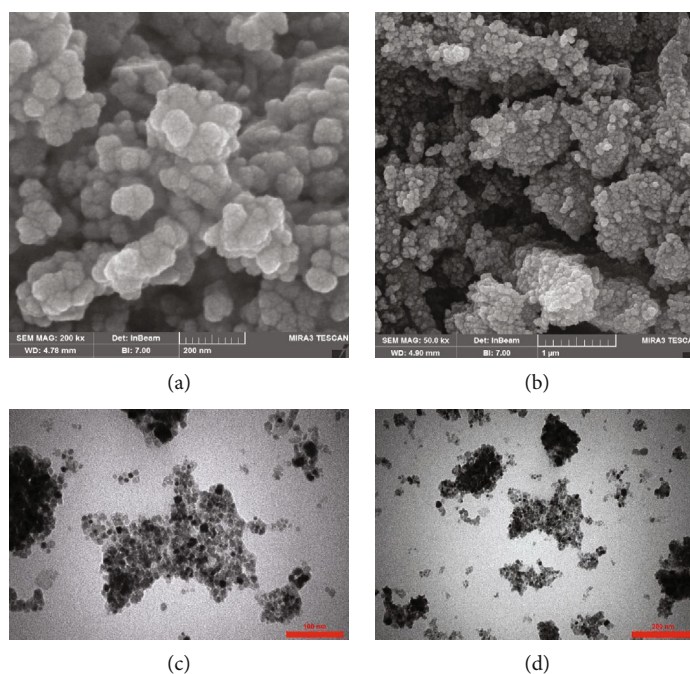


FIGURE 3: The FESEM (a and b) and TEM images (c and d) of green-synthesized AgNPs by *H. elongate*.

the crystalline nature of these AgNPs with a face-centered cubic (fcc) structure. All peaks match with the JCPDS database card No. 04-0783. As shown in Figure 1(b), no additional peaks were observed in the XRD pattern, which confirms the purity of the green-synthesized AgNPs. The highest was found corresponding to the plane (111); thus, this will be the preferred orientation of the cubic structure.

The FTIR spectra of the green-synthesized AgNPs in the range of 400-4000 cm^{-1} are shown in Figure 2. The peaks observed at 3413 and 1591 cm^{-1} correspond to OH and C=O groups, which may be related to bacterial proteins. The peak at 624 cm^{-1} indicates the -CH bond of amino acids in the proteins. The FTIR analysis provides evidence of protein coating on the surface of green-synthesized AgNPs. This means that the proteins in the bacterial extract have more

affinity to bind with Ag^+ ions and act as capping and stabilizing agents, thus reducing the aggregation of produced AgNPs [25, 26]. The peaks in the range of 1380-1410 cm^{-1} belong to strong S=O stretching for sulfonyl chloride [27]. In addition, a band at 1117 cm^{-1} is due to the C-N stretch of aliphatic amines. The peak at 523 cm^{-1} may be due to the presence of Ag-O or pure AgNPs [28].

The morphological and structural features of the green-synthesized AgNPs from *H. elongate*, studied by the FESEM images (Figures 3(a) and 3(b)), showed a high density of green-synthesized AgNPs. According to this analysis, the green-synthesized AgNPs with crystalline nature represented nearly spherical morphology with some aggregates. Images showed that the size of AgNPs ranged between 10 and 80 nm. Furthermore, the TEM images (Figures 3(c)

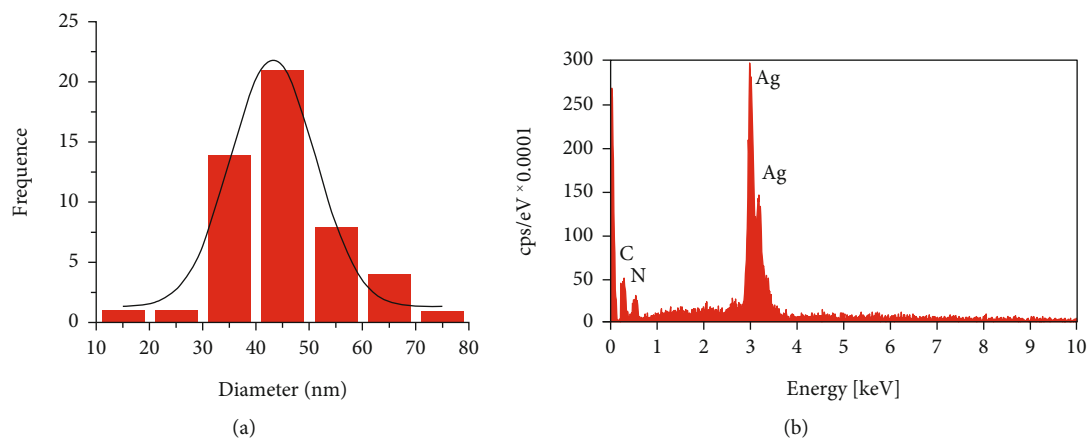


FIGURE 4: (a) Histogram of particle size distribution curve and (b) EDX spectrums of green-synthesized AgNPs by *H. elongate*.

and 3(d)) confirmed the spherical (mostly) and cubic morphologies of the prepared AgNPs. Larger particles are observed from the aggregation of small particles, which may be due to small amounts of observed biological agents or proteins on the surface of AgNPs. Based on the microscopic analyses and the size distribution histogram of green-synthesized AgNPs (Figure 4(a)), the average diameter of nanoparticles was 45 nm. The EDX analysis (Figure 4(b)) revealed the presence of the constituent elements and the purity of the AgNPs produced by green synthesis. These elements included a high amount of silver (80.62%w) and low amounts of carbon (14.75%w) and nitrogen (4.64%w).

4. Conclusion

In the current study, the Taguchi method was applied to optimize the green synthesis process of AgNPs using *H. elongate* as a nonpathogenic bacterial material. At optimal conditions, various techniques (UV-vis, XRD, FTIR, FESEM, and TEM) were used to characterize these NPs. The antibacterial effects of green-synthesized AgNPs were also evaluated against the *S. mutans* biofilm as the famous pathogen of dental caries based on the CFU. The average diameter of these NPs with the most spherical shape measured 45 nm. According to the results of this study, green-synthesized AgNPs in optimal conditions showed higher antibacterial effects. The result confirmed the effective function of these NPs as antibacterial or antibiofilm agents. Therefore, these NPs can be used in dentistry, especially in the treatment of oral infections or dental caries.

Data Availability

The data used to support the findings of this study are included within the article.

Conflicts of Interest

The authors declare that they have no conflicts of interest.

Acknowledgments

The authors gratefully acknowledge the Research Council of Kermanshah University of Medical Sciences (Grant number 990309) for the financial support.

References

- [1] H. R. Mozaffari, E. Zavattaro, A. Abdollahnejad et al., "Serum and salivary IgA, IgG, and IgM levels in oral lichen planus: a systematic review and meta-analysis of case-control studies," *Medicina*, vol. 54, no. 6, p. 99, 2018.
- [2] H. R. Mozaffari, M. Payandeh, M. Ramezani, M. Sadeghi, M. Mahmoudiahmadabadi, and R. Sharifi, "Efficacy of palifermin on oral mucositis and acute GVHD after hematopoietic stem cell transplantation (HSCT) in hematology malignancy patients: a meta-analysis of trials," *Współczesna Onkologia*, vol. 21, no. 4, pp. 299–305, 2017.
- [3] M. Safaei, M. Taran, M. M. Imani et al., "Application of Taguchi method in the optimization of synthesis of cellulose-MgO bionanocomposite as antibacterial agent," *Polish Journal of Chemical Technology*, vol. 21, no. 4, pp. 116–122, 2019.
- [4] M. Huq, "Green synthesis of silver nanoparticles using *Pseudoduganella eburnea* MAHUQ-39 and their antimicrobial mechanisms investigation against drug resistant human pathogens," *International Journal of Molecular Sciences*, vol. 21, no. 4, p. 1510, 2020.
- [5] M. Safaei, M. Taran, L. Jamshidy et al., "Optimum synthesis of polyhydroxybutyrate- Co_3O_4 bionanocomposite with the highest antibacterial activity against multidrug resistant bacteria," *International Journal of Biological Macromolecules*, vol. 158, pp. 477–485, 2020.
- [6] A. Meinen, A. Reuss, N. Willrich et al., "Antimicrobial resistance and the spectrum of pathogens in dental and oral-maxillofacial infections in hospitals and dental practices in Germany," *Frontiers in Microbiology*, vol. 12, p. 1418, 2021.
- [7] J. P. Loyola-Rodriguez, M. E. Ponce-Diaz, A. Loyola-Leyva et al., "Determination and identification of antibiotic-resistant oral streptococci isolated from active dental infections in adults," *Acta Odontologica Scandinavica*, vol. 76, no. 4, pp. 229–235, 2018.
- [8] W. Song and S. Ge, "Application of antimicrobial nanoparticles in dentistry," *Molecules*, vol. 24, no. 6, p. 1033, 2019.

- [9] E. T. Enan, A. A. Ashour, S. Basha, N. H. Felemban, and S. M. F. Gad El-Rab, "Antimicrobial activity of biosynthesized silver nanoparticles, amoxicillin, and glass-ionomer cement against *Streptococcus mutans* and *Staphylococcus aureus*," *Nanotechnology*, vol. 32, no. 21, article 215101, 2021.
- [10] H. Moradpoor, M. Safaei, F. Rezaei et al., "Optimisation of cobalt oxide nanoparticles synthesis as bactericidal agents," *Open access Macedonian journal of medical sciences*, vol. 7, no. 17, pp. 2757–2762, 2019.
- [11] H. Moradpoor, M. Safaei, H. R. Mozaffari et al., "An overview of recent progress in dental applications of zinc oxide nanoparticles," *RSC Advances*, vol. 11, no. 34, pp. 21189–21206, 2021.
- [12] A. Lateef, I. A. Adelere, E. B. Gueguim-Kana, T. B. Asafa, and L. S. Beukes, "Green synthesis of silver nanoparticles using keratinase obtained from a strain of *Bacillus safensis* LAU 13," *International Nano Letters*, vol. 5, no. 1, pp. 29–35, 2015.
- [13] A. Chahardoli, N. Karimi, and A. Fattahi, "Nigella arvensis leaf extract mediated green synthesis of silver nanoparticles: their characteristic properties and biological efficacy," *Advanced Powder Technology*, vol. 29, no. 1, pp. 202–210, 2018.
- [14] B. S. Surendra, C. Mallikarjunaswamy, S. Pramila, and N. D. Rekha, "Bio-mediated synthesis of ZnO nanoparticles using *Lantana camara* flower extract: its characterizations, photocatalytic, electrochemical and anti-inflammatory applications," *Environmental Nanotechnology, Monitoring & Management*, vol. 15, article 100442, 2021.
- [15] B. S. Surendra, T. Kiran, M. V. Chethana, H. S. Savitha, and M. S. Paramesh, "Cost-effective Aegle marmelos extract-assisted synthesis of ZnFe₂O₄: Cu²⁺ NPs: photocatalytic and electrochemical sensor applications," *Journal of Materials Science: Materials in Electronics*, vol. 32, no. 20, pp. 25234–25246, 2021.
- [16] C. Wang, Y. J. Kim, P. Singh, R. Mathiyalagan, Y. Jin, and D. C. Yang, "Green synthesis of silver nanoparticles by *Bacillus methylotrophicus*, and their antimicrobial activity," *Artificial Cells, Nanomedicine, and Biotechnology*, vol. 44, no. 4, pp. 1–6, 2016.
- [17] T. Mustapha, N. Misni, N. R. Ithnin, A. M. Daskum, and N. Z. Unyah, "A review on plants and microorganisms mediated synthesis of silver nanoparticles, role of plants metabolites and applications," *International Journal of Environmental Research and Public Health*, vol. 19, no. 2, p. 674, 2022.
- [18] K. Divya, L. C. Kurian, S. Vijayan, and J. Manakulam Shaikmoideen, "Green synthesis of silver nanoparticles by *Escherichia coli*: analysis of antibacterial activity," *Journal of Water and Environmental Nanotechnology*, vol. 1, no. 1, pp. 63–74, 2016.
- [19] K. I. Alsamhary, "Eco-friendly synthesis of silver nanoparticles by *Bacillus subtilis* and their antibacterial activity," *Saudi Journal of Biological Sciences*, vol. 27, no. 8, pp. 2185–2191, 2020.
- [20] S. M. Aziz Mousavi, S. A. Mirhosseini, M. Rastegar Shariat Panahi, and H. Mahmoodzadeh Hosseini, "Characterization of biosynthesized silver nanoparticles using *Lactobacillus rhamnosus* gg and its in vitro assessment against colorectal cancer cells," *Probiotics and Antimicrobial Proteins*, vol. 12, no. 2, pp. 740–746, 2020.
- [21] H. Zhang, T. Li, W. Luo, G. X. Peng, and J. Xiong, "Green synthesis of Ag nanoparticles from *Leucos aspera* and its application in anticancer activity against alveolar cancer," *Journal of Experimental Nanoscience*, vol. 17, no. 1, pp. 47–60, 2022.
- [22] I. X. Yin, O. Y. Yu, I. S. Zhao et al., "Developing biocompatible silver nanoparticles using epigallocatechin gallate for dental use," *Archives of Oral Biology*, vol. 102, pp. 106–112, 2019.
- [23] Z. Tavaf, M. Tabatabaei, A. Khalafi-Nezhad, and F. Panahi, "Evaluation of antibacterial, antibiofilm and antioxidant activities of synthesized silver nanoparticles (AgNPs) and casein peptide fragments against *Streptococcus mutans*," *European Journal of Integrative Medicine*, vol. 12, pp. 163–171, 2017.
- [24] Á. Martínez-Robles, J. Loyola-Rodríguez, N. Zavala-Alonso et al., "Antimicrobial properties of biofunctionalized silver nanoparticles on clinical isolates of *Streptococcus mutans* and its serotypes," *Nanomaterials*, vol. 6, no. 7, p. 136, 2016.
- [25] F. Jalilian, A. Chahardoli, K. Sadrajavadi, A. Fattahi, and Y. Shokoohinia, "Green synthesized silver nanoparticle from *Allium ampeloprasum* aqueous extract: characterization, antioxidant activities, antibacterial and cytotoxicity effects," *Advanced Powder Technology*, vol. 31, no. 3, pp. 1323–1332, 2020.
- [26] M. Saravanan, S. K. Barik, D. Mubarak Ali, P. Prakash, and A. Pugazhendhi, "Synthesis of silver nanoparticles from *Bacillus brevis* (NCIM 2533) and their antibacterial activity against pathogenic bacteria," *Microbial Pathogenesis*, vol. 116, pp. 221–226, 2018.
- [27] M. M. Al-Ansari, N. D. Al-Dahmash, and A. J. A. Ranjitsingh, "Synthesis of silver nanoparticles using gum Arabic: evaluation of its inhibitory action on *Streptococcus mutans* causing dental caries and endocarditis," *Journal of Infection and Public Health*, vol. 14, no. 3, pp. 324–330, 2021.
- [28] I. A. Wani, "Review—recent advances in biogenic silver nanoparticles and nanocomposite based plasmonic-colorimetric and electrochemical sensors," *ECS Journal of Solid State Science and Technology*, vol. 10, no. 4, article 047003, 2021.